NASA TM X-56

TECHNICAL MEMORANDUM
X - 56

THE EFFECT OF CAMBER ON THE AERODYNAMIC CHARACTERISTICS OF A BODY AT A MACH NUMBER OF 2.01

By John P. Gapcynski

Langley Research Center
Langley Field, Va.

Declassified June 24, 1960

NATIONAL AERONAUTICS AND SPACE ADMINISTRATION

WASHINGTON September 1959

copy 1

Code 1

NATIONAL AERONAUTICS AND SPACE ADMINISTRATION

TECHNICAL MEMORANDUM X-56

THE EFFECT OF CAMBER ON THE AERODYNAMIC CHARACTERISTICS OF A BODY AT A MACH NUMBER OF 2.01

By John P. Gapcynski

SUMMARY

An investigation has been conducted in the Langley 4- by 4-foot supersonic pressure tunnel to determine the effect of camber on the aerodynamic characteristics of an ogive-circular-cylinder type of body with a fineness ratio of 10. Three types of camber were considered: the first being a simple body nose droop of 4°, and the second and third being distortions such that the body center lines had, respectively, circular-arc and reflexed circular-arc shapes. Both force and pressure measurements were obtained on the models at a Mach number of 2.01, a Reynolds number per foot of 3.46×10^{6}, and for an angle-of-attack range of $\pm 10^{\circ}$.

The use of camber resulted in pronounced changes in the body pitch characteristics. Drooping or lowering the nose of the body introduced a negative increment in the pitching-moment variation (pitch center at body midpoint) with little change in the normal-force values. Drooping the rear portion of the body as well as the nose resulted in still more negative pitching-moment increments but positive normal-force increments. The use of nose droop with a raised afterbody resulted in positive pitching-moment increments and negative normal-force increments. Fairly good predictions of the trend and order of magnitude of these pitch characteristics were possible with the application of slender-body theory.

Minimum drag values for the bodies with the drooped nose and circular-arc center line were higher than that of the uncambered body. Little or no increase was noted for the body with the reflexed circular-arc center line.

INTRODUCTION

The use of cambered fuselages in many of the present-day high-speed aircraft has emphasized the need for a knowledge of the effects of camber on the aerodynamic characteristics of bodies and wing-body combinations. The use of body camber may be the result of practical design considerations associated with landing and visibility problems. It has also been noted (refs. 1 and 2) that body camber may be used to produce positive increments in pitching moment with little increase in drag; thereby the required control deflections and associated losses in trim lift-drag ratios are reduced. Of further interest is the applicability of a knowledge of camber effects to the changes in loading, due to structural deformations, of high-fineness-ratio missile configurations. The purpose of this paper is to discuss the results of a detailed investigation of the effects of camber on the aerodynamic characteristics of bodies.

Four bodies were used for this program. The reference body was an ogive-circular cylinder with a fineness ratio of 10. The three additional bodies had basically the same longitudinal area distribution as the reference body but different types of camber, the first having a bent or drooped nose, the second, a circular-arc center line and the third, a reflexed circular-arc center line. Both force and pressure measurements were obtained on these bodies in the Langley 4- by 4-foot supersonic pressure tunnel at a Mach number of 2.01 and for an angle-of-attack range of $\pm 10^{\circ}$. The results are compared with an analysis based on slender-body theory.

SYMBOLS

α	angle of attack (in plane of camber)
q	free-stream dynamic pressure
l	body length
d	body diameter (maximum)
θ	body polar angle
r	local radius of body
S	body cross-sectional area
h	maximum camber of body center line

x distance from apex of body

L/D lift-drag ratio

c_n body section normal-force coefficient, $\frac{\text{Body section normal force}}{2qr}$

C_N body normal-force coefficient, $\frac{\text{Body normal force}}{qS_{max}}$

$C_{m\ell/2}$ body pitching-moment coefficient (about body midpoint), $\frac{\text{Body pitching moment}}{qS_{max}\ell}$

C_L body lift coefficient, $\frac{\text{Body lift force}}{qS_{max}}$

C_D body drag coefficient, $\frac{\text{Body drag force}}{qS_{max}}$

Subscript:

max maximum

DESCRIPTION OF MODELS AND TESTS

Sketches of the models are shown in figure 1. The basic or reference configuration, designated as body 1, was an ogive-circular cylinder with a nose fineness ratio of 5 and an overall fineness ratio of 10. The three additional body shapes used in this investigation were basically similar to the reference body with respect to cross-sectional area distribution but differed in the camber of the body center line. The nose of body 2 was bent downward at an angle of 4° with respect to the rear or cylindrical portion of the body. Body 3 had a circular-arc center line with a maximum camber of 2.6 percent of the body length. Body 4 had a reflexed circular-arc center line of the same radius of curvature as that of body 3. Both force and pressure models of each body shape were constructed to the dimensions given in figure 1. At each of the orifice stations on the pressure models (10 stations for bodies 1, 3, and 4, and 13 stations for body 2), there were 13 orifices located 15° apart from 0° to 180°.

Force and pressure measurements were obtained on these bodies in the Langley 4- by 4-foot supersonic pressure tunnel at a Mach number

of 2.01 and a Reynolds number per foot of 3.46×10^6. The angle-of-attack range was $\pm 10^\circ$. Force data (obtained from an internal strain-gage balance) were obtained for angle-of-attack increments of 1° and pressure data for increments of 2°. The 0° angle-of-attack reference line is shown for each model in figure 1. One-quarter-inch-wide transition strips, consisting of No. 60 carborundum grains set in shellac, were installed one-half inch back from the nose of each model.

Tunnel stagnation conditions were as follows: temperature, 100° F; dewpoint, approximately -35° F; and pressure, 14 lb/sq in. absolute.

PRESENTATION AND DISCUSSION OF RESULTS

The normal-force loading distributions for each body, as determined from pressure measurements, are presented in figure 2. The variation of body lift coefficient with angle of attack and the variations of the moment coefficient (about the midpoint of the body), the drag coefficient, and the lift-drag ratio with lift coefficient are presented in figures 3, 4, 5, and 6, respectively. These data were obtained from the force-test results. The estimated accuracy of these force data is as follows:

C_L	± 0.009
C_D	± 0.005
C_m	± 0.001

It should be noted here that the integrated results of the pressure measurements were not in exact agreement with the force-test results. The trend and order of magnitude of the two sets of data were identical, but the slopes of the curves differed somewhat. Since this difference was not consistent throughout the tests, it was assumed that the differences were due to inaccuracies in the pressure measurements.

Normal-Force Distribution

From an examination of the normal-force loadings presented in figure 2, it is apparent that camber has a pronounced effect on the pitch characteristics of a body. Two points in particular should be emphasized; first, the effect of the bend or break in the contour of body 2 on the normal-force distribution of that body, and second, the rather large effect that the loading on the rear portion of the body has on the moment of bodies 3 and 4.

The loadings on body 1 are typical of the type encountered on an ogive-circular cylinder. Drooping the nose of such a configuration does not change the basic loading over the forward portion (for equivalent angles of attack) but does introduce a region of positive loading on the body in the vicinity of the bend. This positive increment in loading is evident throughout the angle-of-attack range, and is responsible for the unusual changes in the pitch characteristics resulting from this type of body deformation. For example, at a designated angle of attack of 0° the nose of body 2 is bent downward at an angle of 4° with respect to the airstream. The normal-force loading on the forward portion of this body is thus equivalent to that on an uncambered ogive at an angle of attack of -4°. Due to the existence of the positive loading increment in the vicinity of the body midpoint, which in this case is about equal in magnitude to the loading over the nose, there is little if any change in the overall body normal force but a substantial change in the pitching moment.

The load distributions for bodies 3 and 4 indicate that the use of camber may have a rather large effect on the loading over the rear portion of a body. For example, at a designated angle of attack of 10°, the rear portion of body 3 is subject to a large percentage of the overall positive normal force of this configuration. This is in direct contrast to the poor load-carrying ability of an uncambered circular cylinder such as the rear portion of body 1. The normal-force loading for the same region of body 4, on the other hand, becomes negative even though the body itself is at a positive angle of attack.

Total-Force Coefficients

The effects of camber on the overall force characteristics of an ogive-circular-cylinder type of body are shown in figures 3 to 6. Drooping the nose of this configuration has very little effect on the lift (fig. 3) at the lower angles of attack but does introduce a negative increment in pitching moment (fig. 4). At the higher angles of attack, due to the change in magnitude of the viscous crossflow effects between the two bodies, there is an effect of nose droop on the lift as well as on the moment variation. If both the nose and the rear portion of the body are bent downward (a configuration corresponding to body 3), there is a positive shift in the normal force and a further increase in the negative pitching moment. The use of nose droop with a raised afterbody (a configuration corresponding to body 4) results in a negative shift in the normal-force variation with a pronounced positive shift in the pitching-moment variation.

The effect of body camber on the drag characteristics is shown in figures 5 and 6. In each case, the use of camber resulted in an increase

in minimum drag, the largest increase occurring with the body having a circular-arc center line (body 3) and the smallest increase occurring with the body having a reflexed circular-arc center line (body 4).

For the same values of negative lift coefficient, the drag values of bodies 2 and 3 are higher than that of the uncambered body, whereas the drag of body 4 is approximately the same as that of the uncambered body. For the larger positive lift coefficients, the exact opposite is true; that is, body 4 has the higher drag values.

If the results of this investigation are viewed from the standpoint of using body camber as a trim-producing mechanism, it is apparent from the preceding discussion that the configurations best suited for this purpose are also those with the increased drag values. The maximum positive increment in pitching moment would be secured by bending both the nose and the rear portion of the body upward. This configuration, however, would have the lowest lift-drag ratio. A smaller increment in pitching moment may be obtained with less decrease in lift-drag ratio by drooping the nose and raising the rear portion of the body. All of these effects, however, could be modified by the presence of a wing.

Theoretical Considerations

In an attempt to estimate the normal forces and pitching moments on these bodies an application of slender-body theory was made. It was assumed that a cambered body in a uniform upwash field may be replaced by an uncambered body in a nonuniform upwash field, the definition of this nonuniform field being obtained from the orientation of the cambered body axis with respect to the free-stream direction. The lift on the body in this nonuniform upwash field then becomes a function of the rate of change of body cross-sectional area and the rate of change of the upwash. As noted in reference 3, if discontinuities exist in the upwash field at points along the body axis, the normal-force distribution will contain concentrated forces at these points. For example, body 2 at an angle of attack of 0° may be considered as an uncambered body immersed in a varying flow field such that the nose is in an upwash field corresponding to an angle of attack of -4°, whereas the rear portion is in an upwash field corresponding to an angle of attack of 0°. At the body midpoint where a discontinuity exists in the upwash field, a concentrated force exists. For the particular case in question, the magnitude of this concentrated force is equal and opposite to overall normal force on the nose since the total normal force on this body at this angle of attack is zero according to slender-body theory. It was pointed out in reference 3 that in the actual case this concentrated force would in all probability be distributed over some finite body length, and from an examination of the loadings in figure 2 it may be seen that this is true.

The comparison of the estimated and experimental variations of body normal-force and pitching-moment coefficients with angle of attack are presented in figures 7 and 8. The estimated values include viscous crossflow effects as determined by the method of reference 4. Although the prediction of absolute magnitudes is not excellent, particularly with respect to pitching moments, the estimations of the trends of the curves are fairly good. This is especially true with regard to the displacement of the curves due to the effect of camber.

CONCLUSIONS

The effects of camber on the aerodynamic characteristics of an ogive-circular-cylinder type of body have been determined at a Mach number of 2.01, a Reynolds number per foot of 3.46×10^6, and for an angle-of-attack range of $\pm 10^\circ$ and are as follows:

1. The use of camber resulted in pronounced changes in the body pitch characteristics. Drooping or lowering the nose of the body introduced a negative increment in the pitching-moment variation (pitch center at body midpoint) with little change in the normal-force values. Drooping the rear portion of the body as well as the nose resulted in still more negative pitching-moment increments but positive normal-force increments. The use of nose droop with a raised afterbody resulted in positive pitching-moment increments and negative normal-force increments. Fairly good predictions of the trend and order of magnitude of these pitch characteristics were possible with the application of slender-body theory.

2. Minimum drag values for the bodies with the drooped nose and circular-arc center line were higher than that of the uncambered body. Little or no increase was noted for the body with the reflexed circular-arc center line.

Langley Research Center,
National Aeronautics and Space Administration,
Langley Field, Va., May 22, 1959.

REFERENCES

1. Spearman, M. Leroy, and Driver, Cornelius: Effects of Forebody Deflection on the Stability and Control Characteristics of a Canard Airplane Configuration With a High Trapezoidal Wing at a Mach Number of 2.01. NASA MEMO 4-4-59L, 1959.

2. Dickey, Robert R.: Effect of Camber on the Drag of a Body of Revolution. NACA RM A56E23, 1956.

3. Gapcynski, John P., and Carlson, Harry W.: The Aerodynamic Characteristics of a Body in the Two-Dimensional Flow Field of a Circular-Arc Wing at a Mach Number of 2.01. NACA RM L57E14, 1957.

4. Allen, H. Julian: Estimation of the Forces and Moments Acting on Inclined Bodies of Revolution of High Fineness Ratio. NACA RM A9I26, 1949.

Symbol	Pressure Model	Force Model
l	24.0	36.0
d	2.4	3.6

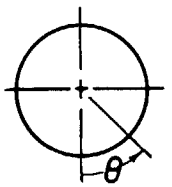

Section A-A

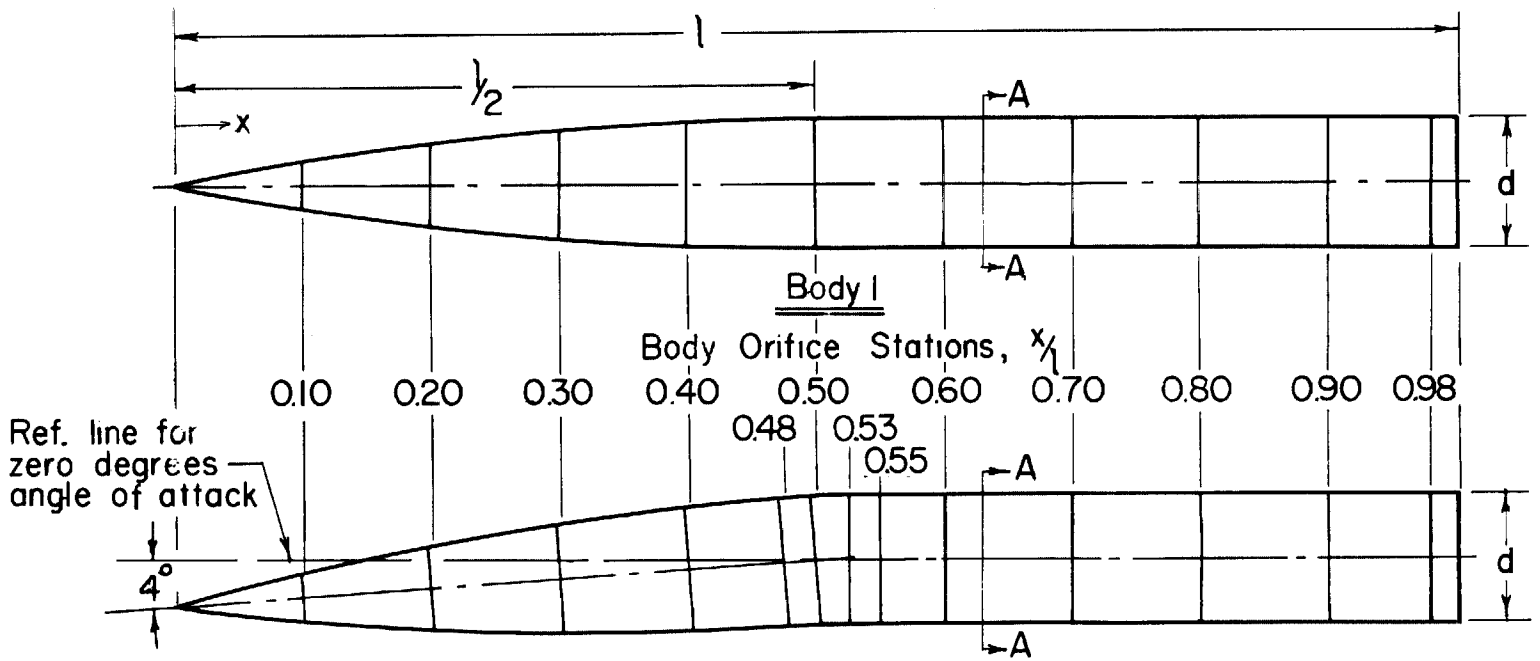

Body 2

Figure 1.- Details of test models.

Symbol	Pressure Model	Force Model
l	24.00	36.00
d	2.40	3.60
h	.63	.94

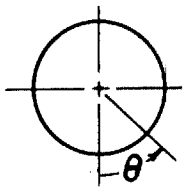

Section A-A

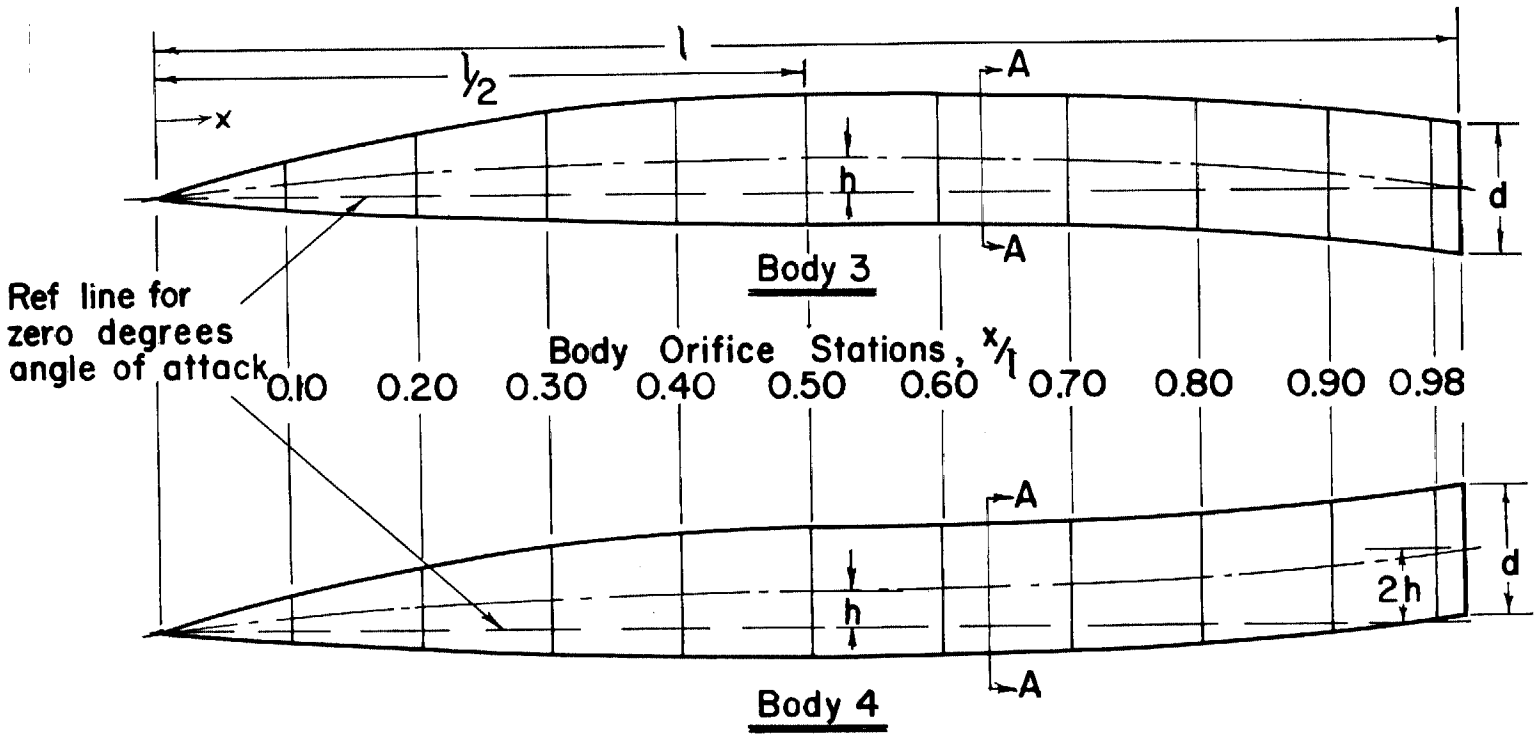

Figure 1.- Concluded.

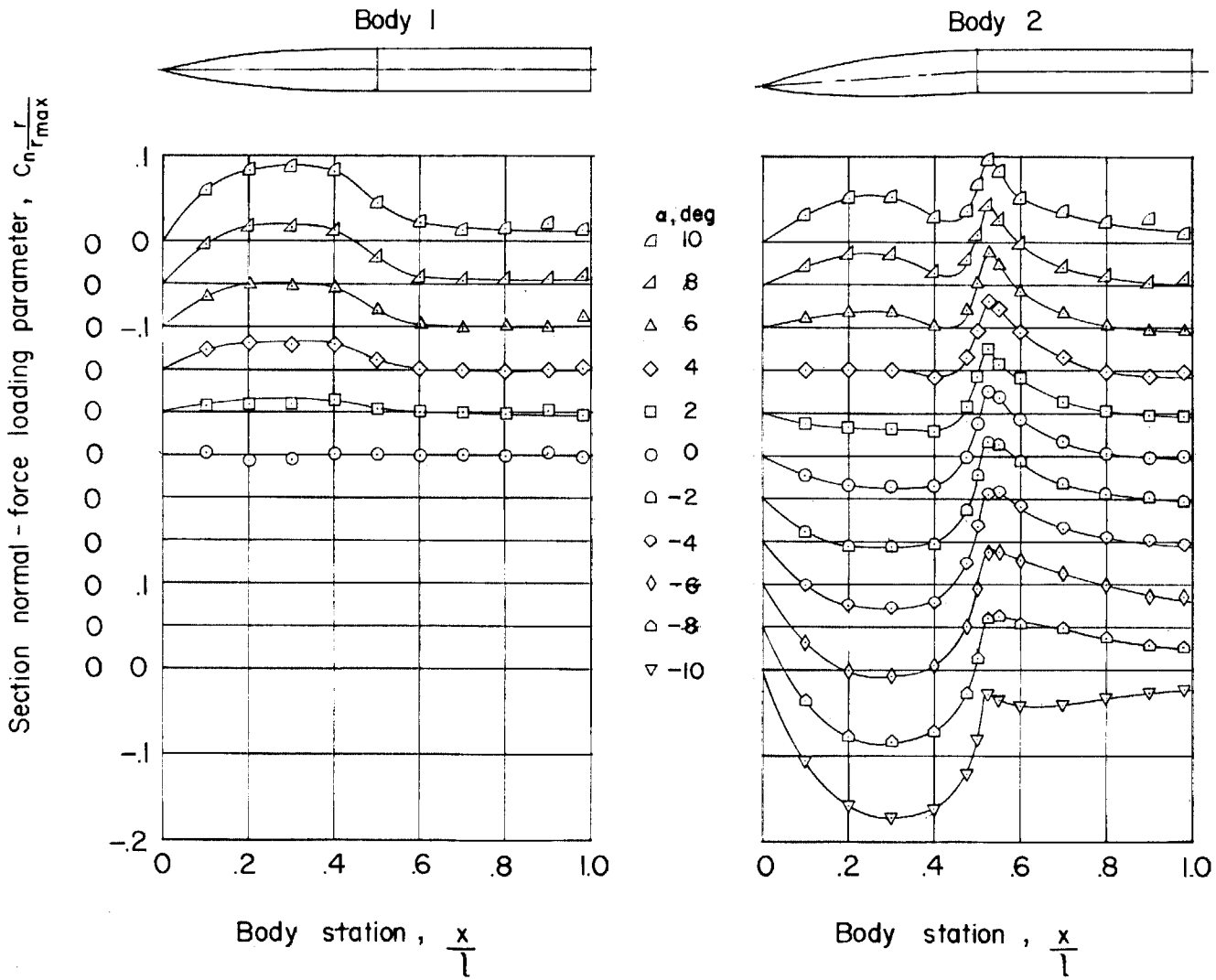

Figure 2.- Normal-force loading distributions on test models.

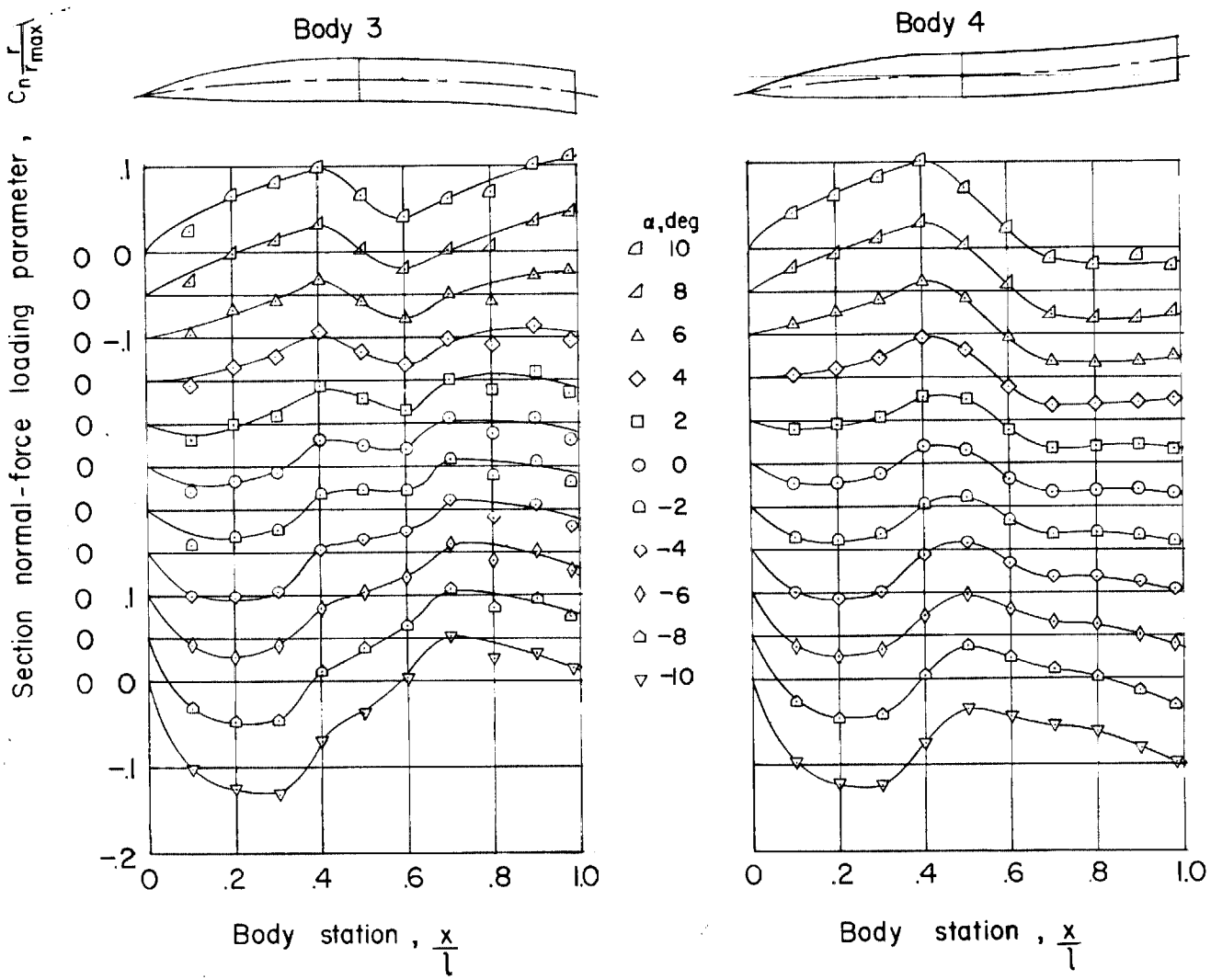

Figure 2.- Concluded.

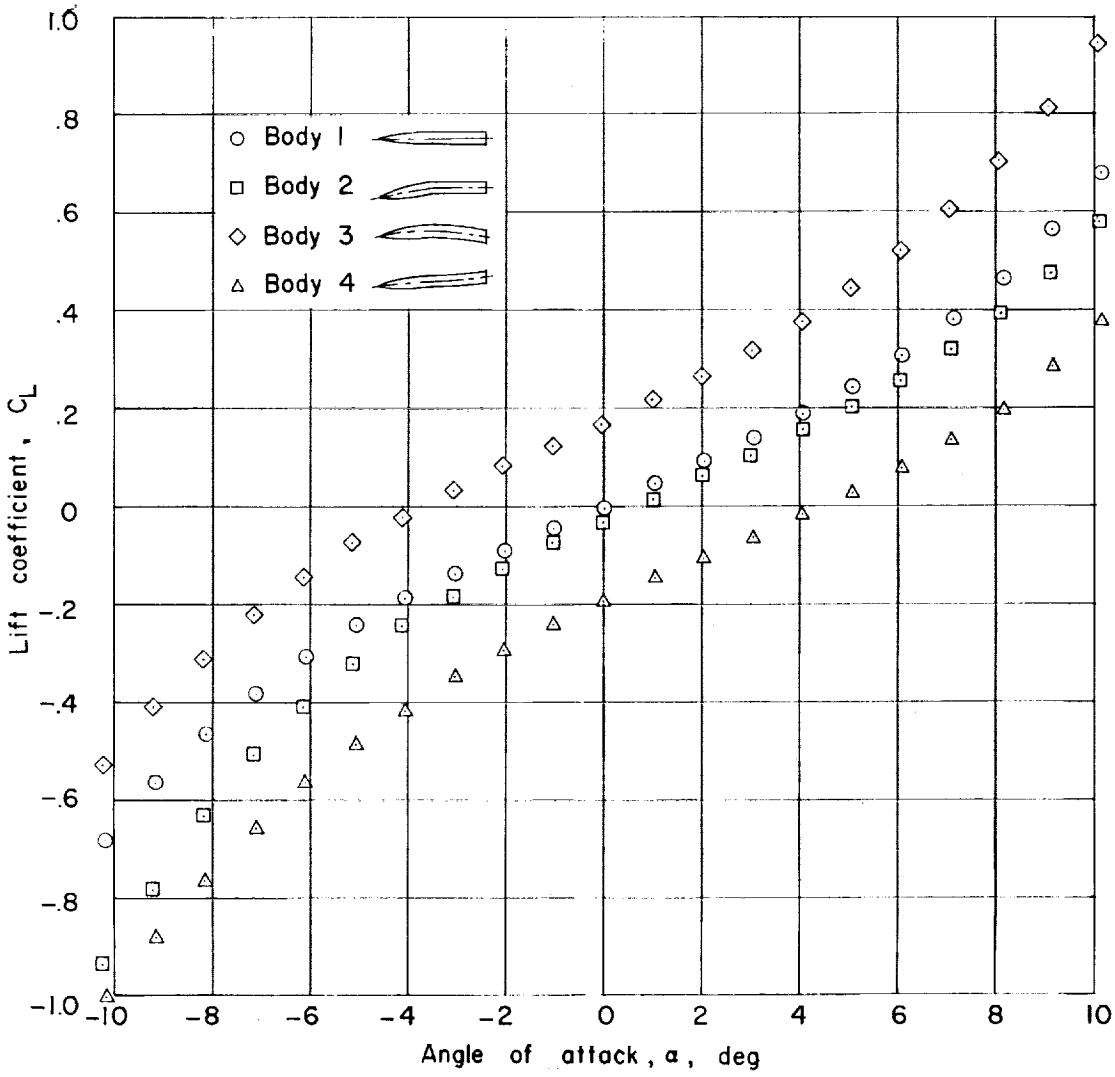

Figure 3.- Variation of body lift coefficient with angle of attack.

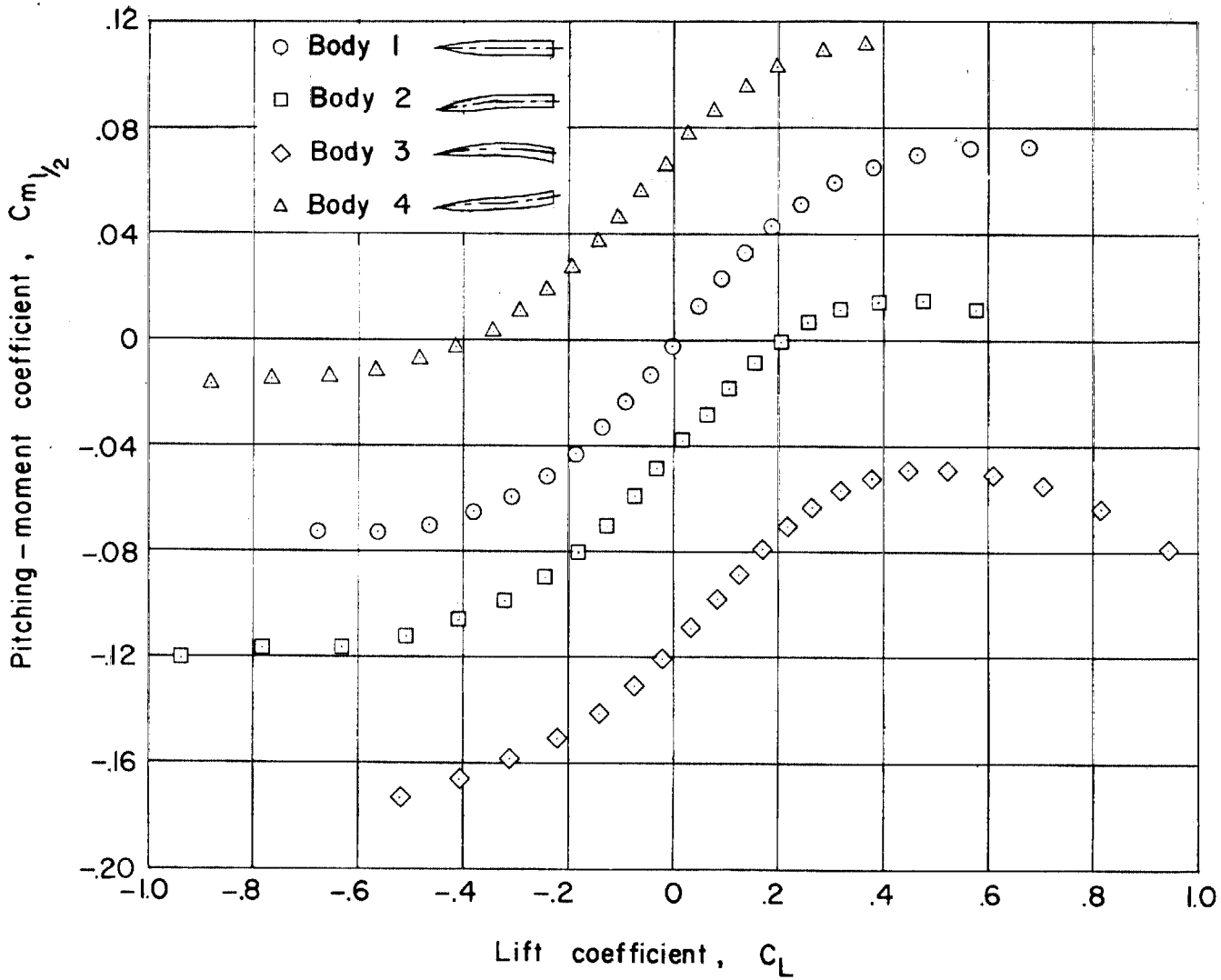

Figure 4.- Variation of body pitching moment (about body midpoint) with body lift coefficient.

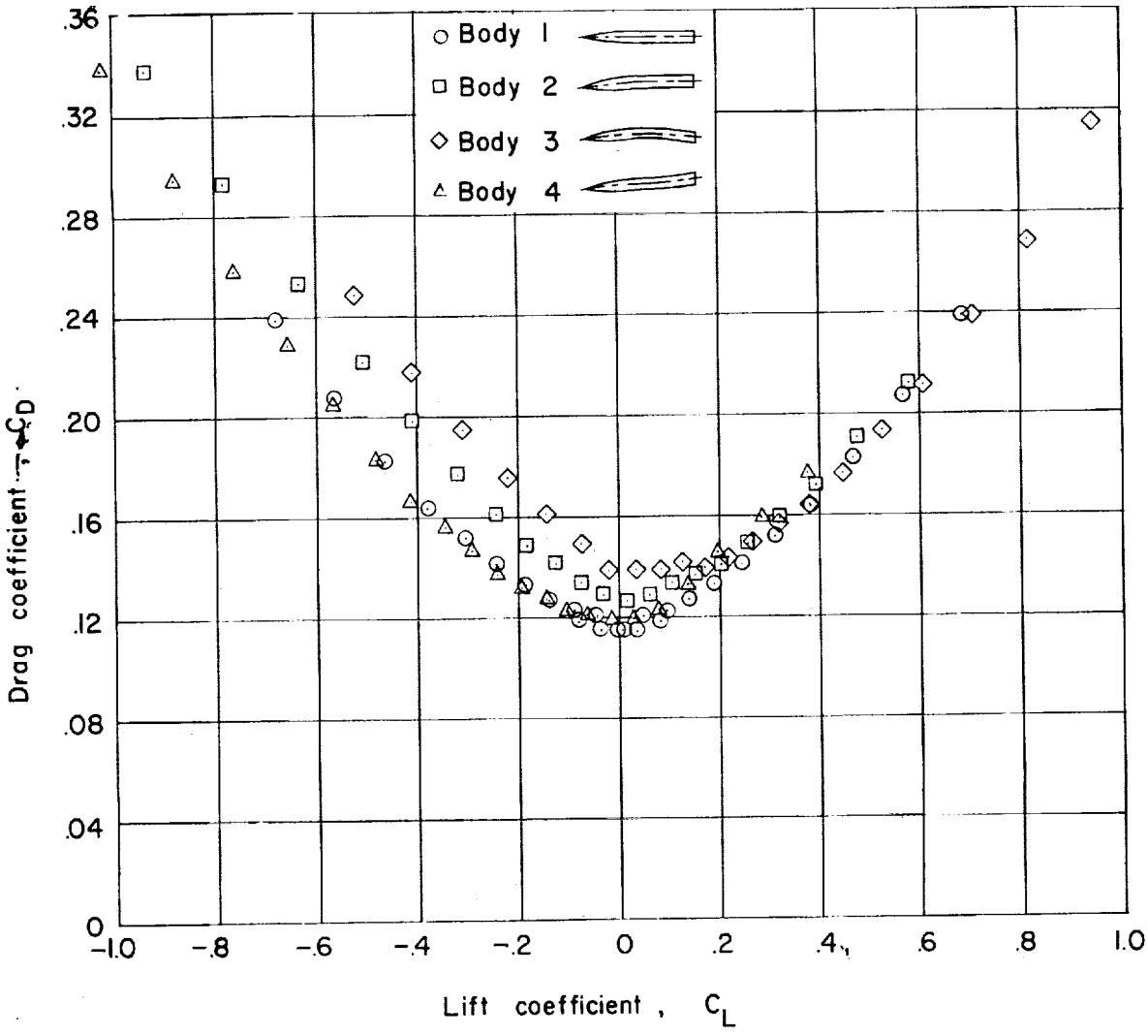

Figure 5 - Variation of body drag coefficient with body lift coefficient.

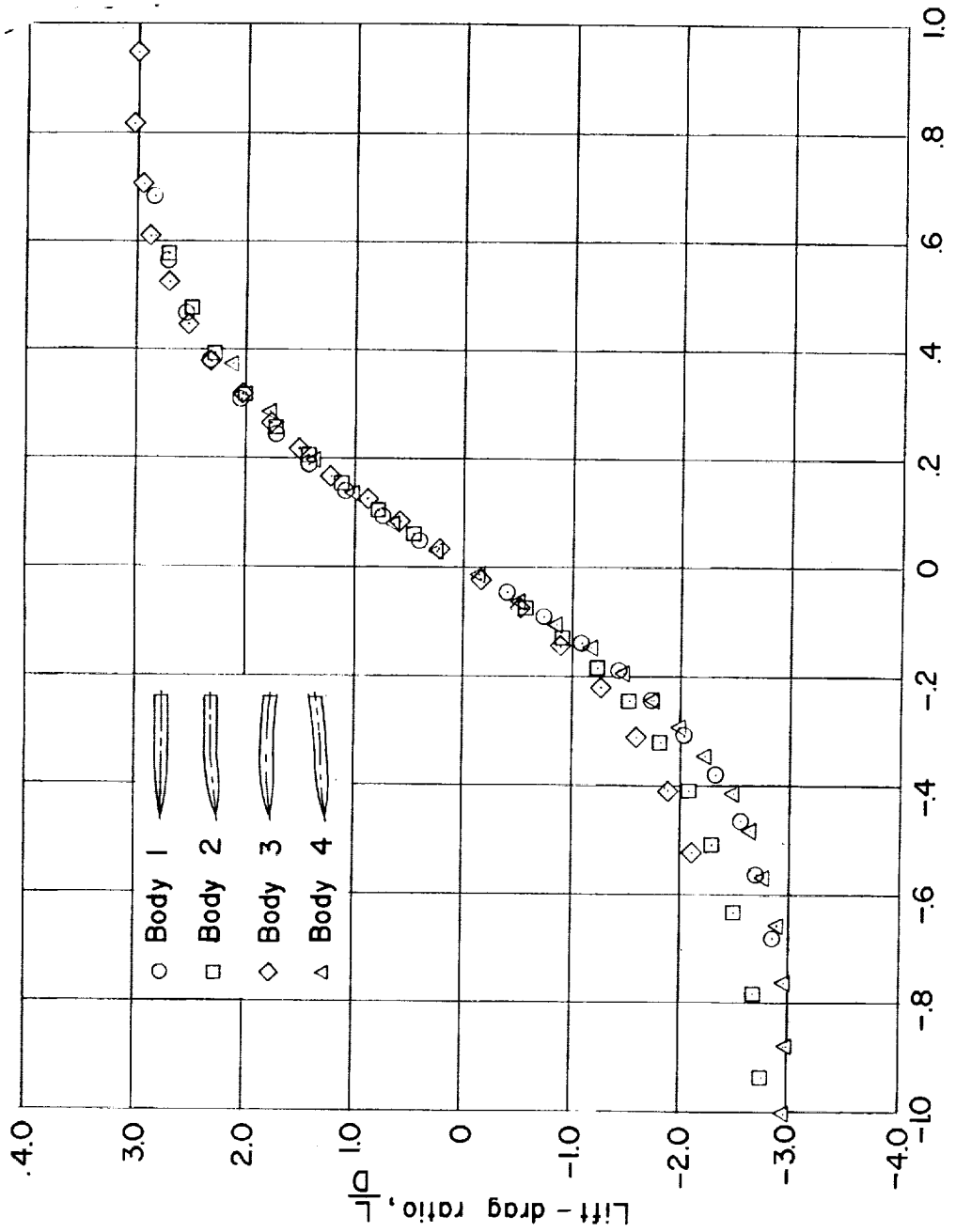

Figure 6.- Variation of body lift-drag ratio with body lift coefficient.

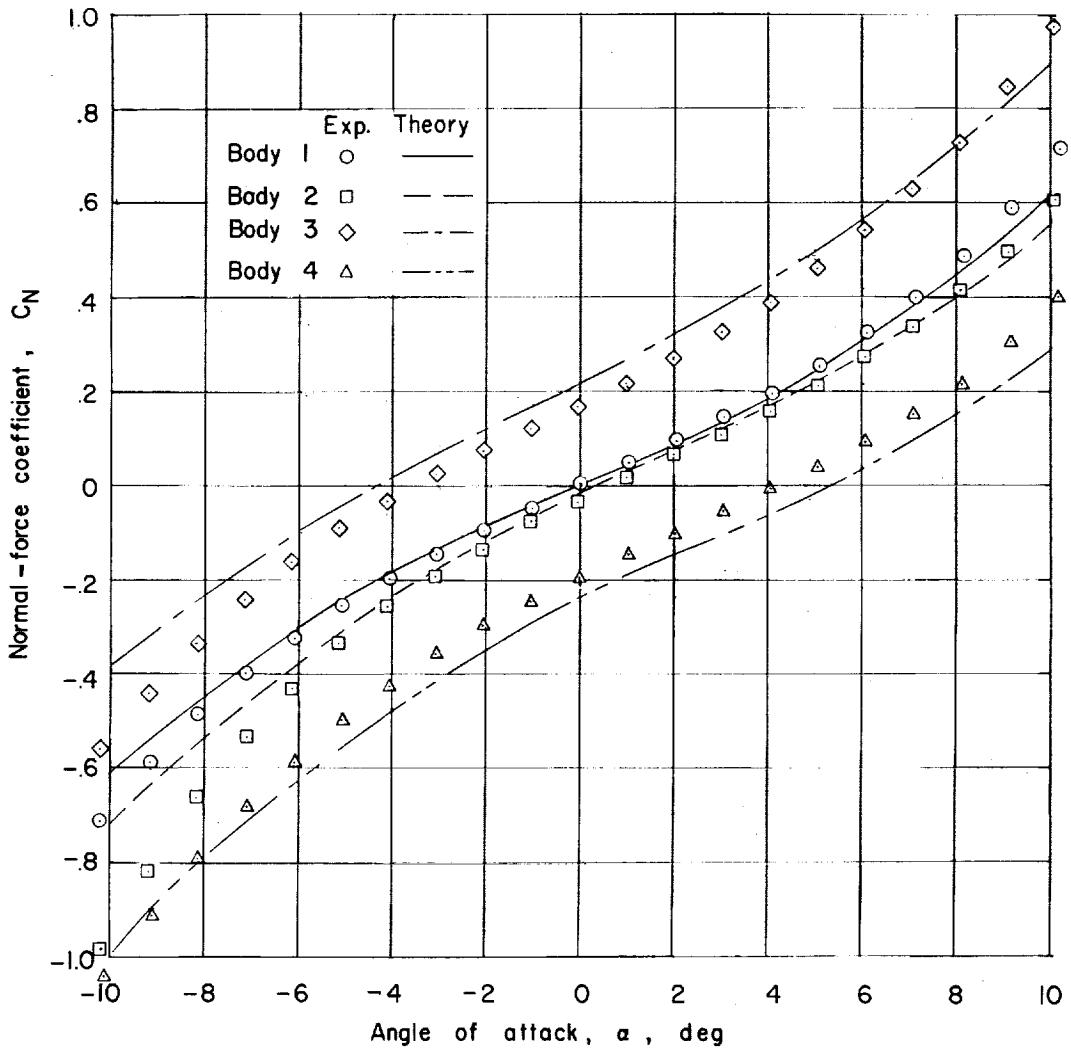

Figure 7.- Comparison between experimental and theoretical variation of body normal-force coefficient with angle of attack.

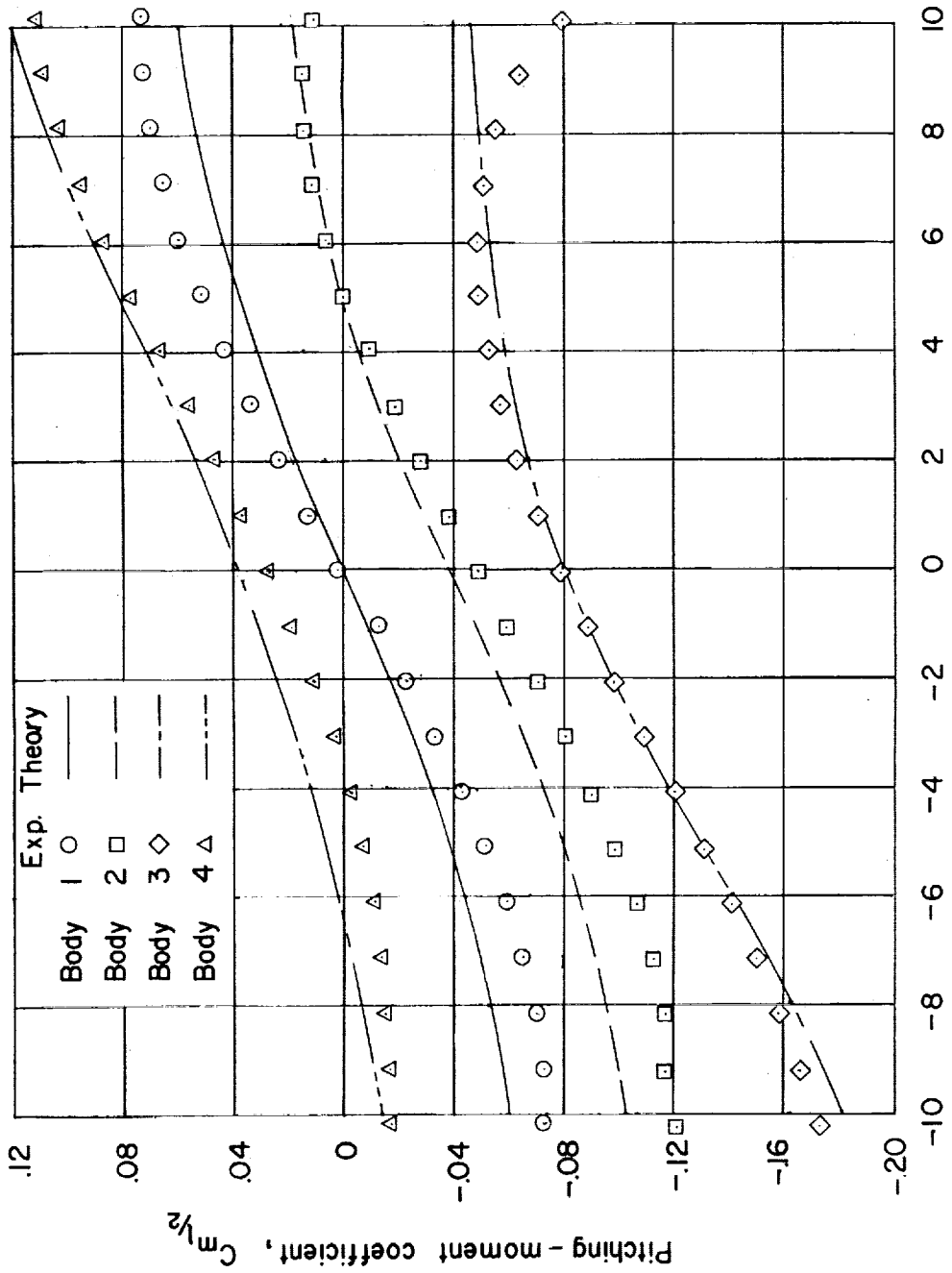

Figure 8.- Comparison between experimental and theoretical variation of body pitching moment with angle of attack.

L-371